MANTECH Publications

Journal of Engineering Mathematics & Statistics
Volume 3, Issue 2, July-December 2019

Solution of Shallow Water Equations using Elliptic Grid System to Predict the Maximum Storm Surges along the Head Bay of Bengal- Application to Cyclone Sidr (2007) and Aila (2009)

Farzana Hussain

Assistant Professor

Department of Mathematics

Huston Tillotson University, Austin, TX, USA

Corresponding Author's Email: *fhussain@htu.edu[1], farzanahsn@gmail.com[2]*

Abstract

A new approach of grid system generation is developed in this study to solve the shallow water equations. A system of straight lines and concentric, uniformly distributed ellipses are considered as the grid lines. Then a stretching along the radial direction is done so that the elliptic arc distant and radial distant between two points is small near the origin which is coarse away from the origin. Using mathematical transformations and appropriate initial/ boundary conditions the transformed shallow wa-ter equations are solved to estimate the water level due to tide and surge associated with some cyclone that hits the coastal region of Bangladesh. This grid system ensures the flexibility of having an optimum shape suitable for representing the coastal and island boundaries by changing the eccentricity of the sys-tem of ellipses and is found to be suitable for incorporation of the bending of the coastline and the isl-and boundaries accurately.

AMS Subject Classifications: *35F30, 37M05, 65N06, 65N50*

Keywords: *Cyclone Sidr, Cyclone Aila, Tropical Storms, Surge, Shallow water equations, Transformation of Coordinates, Bay of Bengal.*

Page 81-103 © MANTECH PUBLICATIONS 2019. All Rights Reserved

NTRODUCTION

The geometry of the coast line of Bay of Bengal is very much complex and curvilinear with high bending, also; there are a lot of small and big islands in the offshore region. The Bay of Bengal is sur-rounded by the coasts from all sides except the southern open sea (Fig. 1). Numerical modeling for prediction of surge due to a storm needs the representation of the coastal geometry accurately. If the grid size is not small in a stair step model the representation of the coastal boundaries is not accurate, where the curvilinear coastal and island boundaries are approximated along the nearest finite difference gridlines [1-9]. A very fine grid resolution near the coast and offshore region is necessary to incorpo-rate the island boundaries and the coastline properly through stair steps, which is not necessary away from the coast. Consideration of very fine resolution involves more computer memory and CPU time in the solution process and invites problem of numerical instability or complexity.

A fine mesh numerical scheme was nested into a coarse mesh scheme in [8] for the Bay of Bengal. In the fine mesh scheme, all the major islands were incorporated through proper stair step representation. This model was similar to [9] for the East Coast of India and the coast of Bangladesh. Recently [5-7] developed some models using nested numerical models. In [5] a fine mesh scheme incorporating the coastal belt and islands has been nested in to a coarse mesh scheme covering up to 15o N latitude in the Bay of Bengal. In the fine mesh scheme, all the major islands are incorporated through proper stair step representation.

Again, a very fine mesh scheme for the region between Barishal and Chittagong is again nested in to the fine mesh scheme. [6, 7] Simulated water levels for storm “Aila -2009” and “Sidr -2007” using nested numerical scheme. The complexity of the models lies in the matching of the bounda-ry line of the fine mesh and curse mesh scheme within the domain. The effect of presence of river on the surge development is discussed in [10] using boundary fitted stair step models. [11] Developed a storm surge for the Myanmar coast. The expected total water levels for the coast of India, Pakistan are computed in [12 - 14]. In these works, the east-west bounda-ries of the analysis area are considered as straight lines.

Page 81-103 © MANTECH PUBLICATIONS 2019. All Rights Reserved



Figure 1 Path of Cyclone Sidr-2007 (Red line), Aila-2009 (Black line) and analysis area

Source: Bangladesh Space Re-search and Remote Sensing Organization

For the bay of Bengal, the transformed coordinate models were based on representing two opposite boundaries as curvilinear and the rest two, generally along the open sea, as straight ones [15- 20] where none of the offshore islands were incorporated. The main difficulty in incorporating the islands was that, in the transformed domain their boundaries became undetectable. [21] developed a model based on the functions defined for two opposite curved boundaries of the analysis area, one generalized function is derived to represent approximately two opposite boundaries of each island. Mathematical transformations render the whole analysis area in to a square and the islands became rectangles. But the limitation is, if we want to incorporate the coastal and island boundaries accurately in the numerical scheme, the grid size in the physical domain must be reduced. In the recent model [22] the boundary fitted curvilinear grids represents the complete boundaries of the analysis area considered by four functions, generalized functions are developed to represent the boundaries and islands accurately in the model. The major islands were incorporated also. Mathematical transformations were used to transform the whole analysis area in to a square and the islands became rectangles.

Page 81-103 © MANTECH PUBLICATIONS 2019. All Rights Reserved

A Circularl Polar coordinate model is developed in [23]. Considering the funnel shaped Bay of Bengal region, the present study ensures fine resolution near the coast and coarse resolution away from the coast by using a single numerical scheme. In this study the Cartesian coordinate system is considered where the origin, *O*, is at (23° N, 91.25° L) in the mean sea level (MSL). A pencil of straight lines through the origin, *O*, at uniform angular distance is considered as one system of grid lines. A system of concentric ellipses with center at *O* and of constant eccentricity is considered as the other system of grid lines.The flexibility of this grid system is that by changing the eccentricity of the system of ellipses we can have an optimum shape suitable for representing the coastal and island boundaries. It may be observed that, as a particular case, the elliptic grid system becomes circular as the eccentricity vanishes. Obviously the elliptic arc distant between two grid points is small near the origin which is greater away from the origin. A stretching of grid points along radial direction is done so that the radial distant between two grid points is also small near the origin (the coastal region) which is greater away from the origin (open sea region). Thus we can cover a large computational domain with a reduced number of grid points representing the coastal geometry accurately. This stretching technique also reduces the CPU memory and computation time. Mathematical transformation renders the physical domain to rectangular one. Regular explicit finite difference scheme is used to solve the transformed Shallow water equations using appropriate initial and boundary conditions to estimate the water level due to tide and surge. This grid system is found to be very affectively applicable in incorporating the bending of the coastline and the island boundaries with a considerable accuracy in the numerical scheme.

MATHEMATICAL FORMULATION

Vertically integrated shallow water equations

The origin, *O*(23° N, 91.25° L), of the system of rectangular Cartesian coordinate is on the undisturbed level of sea surface (MSL). *Ox*, *Oy* and *Oz* points respectively towards the south, the east and vertically upward. The analysis area lies between $y = m_1x$ and $y = m_2x$ along the positive direction of *x*- axis where $m_1 = \tan\alpha$ and $m_2 = \tan\beta$, with $\beta < 0 < \alpha$ (Fig.2a).

The position of the sea surface and the sea floor are considered as $z = \zeta(x, y, t)$ and $z = -h(x, y)$ respectively. The vertically integrated shallow water equations adopted from [8] are

Page 81-103 © MANTECH PUBLICATIONS 2019. All Rights Reserved

$$\frac{\partial \zeta}{\partial t} + \frac{\partial}{\partial x}\{(\zeta + h)\, u\} + \frac{\partial}{\partial y}\{(\zeta + h)\, v\} = 0 \tag{1}$$

$$\frac{\partial u}{\partial t} + u\frac{\partial u}{\partial x} + v\frac{\partial u}{\partial y} - f\, v = -\, g\frac{\partial \zeta}{\partial x} + \frac{\tau_x}{\rho(\zeta + h)} - \frac{c_f\, u(u^2 + v^2)^{1/2}}{\zeta + h} \tag{2}$$

$$\frac{\partial v}{\partial t} + u\frac{\partial v}{\partial x} + v\frac{\partial v}{\partial y} + f\, u = -\, g\frac{\partial \zeta}{\partial y} + \frac{\tau_y}{\rho(\zeta + h)} - \frac{c_f\, v(u^2 + v^2)^{1/2}}{\zeta + h} \tag{3}$$

In the above equations u and v are the vertically integrated components given by

$$(u,\, v) = \frac{1}{\zeta + h}\int_{-h}^{\zeta} (\bar{u}, \bar{v})\, dz \tag{4}$$

Where, $\bar{u}$ and $\bar{v}$ are *x* and *y* components of the Reynolds averaged velocity.

Using (1) we may express (2) & (3) in the flux form and thus, (1) – (3) may be written as

$$\frac{\partial \zeta}{\partial t} + \frac{\partial \tilde{u}}{\partial x} + \frac{\partial \tilde{v}}{\partial y} = 0 \tag{5}$$

$$\frac{\partial \tilde{u}}{\partial t} + \frac{\partial (u\tilde{u})}{\partial x} + v\frac{\partial (v\tilde{u})}{\partial y} - f\,\tilde{v} = -\, g(\zeta + h)\frac{\partial \zeta}{\partial x} + \frac{\tau_x}{\rho} - \frac{c_f\, \tilde{u}\,(u^2 + v^2)^{1/2}}{\zeta + h} \tag{6}$$

$$\frac{\partial \tilde{v}}{\partial t} + \frac{\partial (u\tilde{v})}{\partial x} + \frac{\partial (v\tilde{v})}{\partial y} + f\,\tilde{u} = -\, g(\zeta + h)\frac{\partial \zeta}{\partial y} + \frac{\tau_y}{\rho} - \frac{c_f\, \tilde{v}\,(u^2 + v^2)^{1/2}}{\zeta + h} \tag{7}$$

where $(\tilde{u}, \tilde{v}) = (\zeta + h)\,(u, v)$. In the last terms of (6) & (7) $\tilde{u}$ and $\tilde{v}$ are considered for applying a semi-implicit numerical integration scheme by keeping them in the advanced time level in the solution process. Further discussion about $\tilde{u}$ and $\tilde{v}$ will follow in the section of numerical solution.

To generate the wind field over the analysis area the empirical formula given by [30] is followed:

$$V_a = V_o (r/R)^{3/2} \quad for \quad r \le R \tag{8}$$
$$= V_o (R/r)^{1/2} \quad for \quad r > R$$

Radial and tangential components of wind stress are derived by

Page 81-103 © MANTECH PUBLICATIONS 2019. All Rights Reserved

$$(\tau_r, \tau_\theta) = C_D \rho_a (u_a^2 + v_a^2)^{1/2} (u_a, v_a) \qquad (9)$$

τ_x and τ_y, the x and y component of wind stress are derived from τ_r and τ_θ.

Boundary Conditions

The normal component of velocity is considered as zero for a closed boundary. For open boundaries the radiation type boundary conditions are considered which allow the disturbance created within the analysis area to go out of the area. The boundary conditions are given by

$$v\cos\alpha - u\sin\alpha = 0 \; or \; +(g/h)^{1/2}\zeta \quad \text{at } y = m_1 x \qquad (10)$$

$$v\cos\beta - u\sin\beta = 0 \; or \; -(g/h)^{1/2}\zeta \quad \text{at } y = m_2 x \qquad (11)$$

$$u\cos\phi + v\sin\phi = (g/h)^{1/2}\zeta \quad \text{at the south boundary} \qquad (12a)$$

For generating tide in the basin the southern open sea boundary condition is taken as

$$u\cos\phi + v\sin\phi = (g/h)^{1/2}\zeta - 2(g/h)^{1/2} \; a \; Sin[(2\pi t)/T + \varphi] \qquad (12b)$$

where a and φ denote respectively the prescribed amplitude and phase of the tidal force and T is the tidal period.

GRID GENERATION

For relatively simple geometry conformal or orthogonal grids may be generated. For most complex estuarine and coastal applications, conformal or orthogonal grids may not be generated. Generally, orthogonal or non-orthogonal curvilinear grid generation is accomplished by solving partial differential equations [25-28]. Transformations of Coordinates equation satisfying some characteristics of curvilinear grids are used to produce mesh by using the variational method in [25]. The Poisson equations are employed to generate non-orthogonal grids in [26]. The idea of coordinate transformation and producing grids by solving two Poisson equations are described in [28]. In the present study a system of non-orthogonal grids are generated based on the intersection of two systems of lines defined by two equations.

Page 81-103 © MANTECH PUBLICATIONS 2019. All Rights Reserved

The study area is bounded by the lines $y = m_1x$ and $y = m_2x$, through origin O (23° N, 91.25° L), and they are inclined to the x- axis at angles $\beta < 0 < \alpha$ respectively so that $m_1 = \tan\alpha$ and $m_2 = \tan\beta$. The angle between $y = m_1x$ and y = m_2x are divided into, say, $N_2 - 1$ equal angles, each equals to $\Delta\theta$, by a pencil of straight lines given by

$$y = m\,x \qquad (13)$$

Thus we have a pencil of N_2 straight grid lines through O including the bounding lines.

A system of concentric ellipses each with center at O, major axis along y-axis, minor axis along x- axis and of constant eccentricity is given by

$$\frac{x^2}{r^2} + \frac{y^2}{R^2} = 1 \qquad (14a)$$

with $r^2 = R^2(1 - e^2)$, where e is the eccentricity of the system. The Eq. (14a) may also be written as

$$\frac{x^2}{1} + \frac{y^2}{c^2} = r^2 \qquad (14b)$$

with $R^2/r^2 = 1/(1 - e^2) = c^2$, where $c > 1$ is a constant so long e is constant and r is the parameter representing the lengths of the semi-minor axes.

Obviously the elliptical arc distant between two grid points is small near the coast which is large away from the coast. If we generate equidistant ellipses with a very fine grid resolution the total number of grid points becomes larger. To represent the coastal geometry properly we need a fine resolution near the coast which is unnecessary away from the coast. So along the radial distant we consider a fine resolution near the coast which is not so away from the coast by taking variable distances between the ellipses. Using this technique we can cover a large domain with reduced number of grid points which reduces the CPU memory, computation time also.

We generate N_1 unevenly spaced ellipses, the ellipse with $r = 0$ is considered for convenient application of finite difference scheme and N_2 grid points meet at O. However, there will be no computation at O and so, there is no possibility of numerical instability in the solution process. Thus we have a 2-D nearly orthogonal grid system with $N_1 \times N_2$ grid points given by

Page 81-103 © MANTECH PUBLICATIONS 2019. All Rights Reserved

$\left(cr/\sqrt{m^2+c^2}, mcr/\sqrt{m^2+c^2}\right)$. It may be noted that as $e \to 0$ the system of ellipses approaches to a system of circles and the grid system approaches to an orthogonal one. The grid system is shown in the Fig.2a.

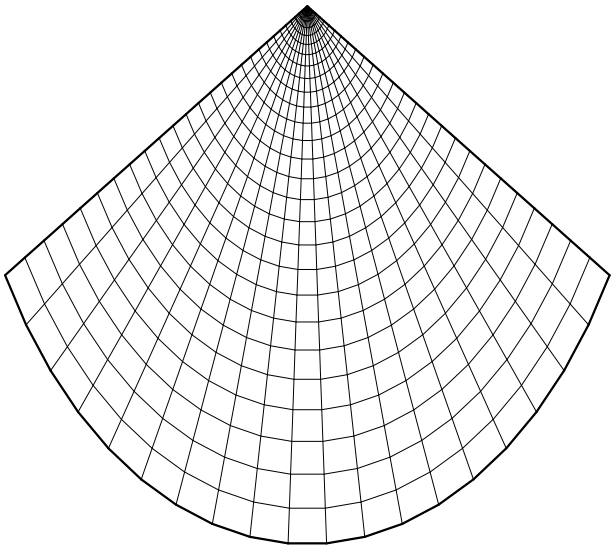


Figure 2a Elliptic grid system in the physical domain.

TRANSFORMATION OF COORDINATES

To facilitate the numerical treatment in the rectangular computational grid system, we introduce transformations based upon a new set of independent variable r, θ and t given by

$$x = r\cos\theta, \quad y = rc\sin\theta \quad \text{where } r \geq 0 \quad \text{and} \quad \beta \leq \theta \leq \alpha \tag{15a}$$

or equivalently

$$r = +\sqrt{x^2 + y^2/c^2}, \quad \theta = arc\tan[y/(cx)] \tag{15b}$$

These transformations transform the physical domain between $y = m_1x$, $y = m_2x$, and the southern elliptic boundary into a rectangular one given by

$$0 \leq r \leq K, \quad \beta \leq \theta \leq \alpha \tag{16}$$

where K is the semi minor axis for the southern elliptic boundary. Also, the curvilinear grid system is transformed to a rectangular grid system in r - θ domain. The grid system in the transformed domain is shown in Fig2b.

The Jacobean of transformation is given by

Page 81-103 © MANTECH PUBLICATIONS 2019. All Rights Reserved

$$J = \begin{vmatrix} \frac{\partial x}{\partial r} & \frac{\partial y}{\partial r} \\ \frac{\partial x}{\partial \theta} & \frac{\partial y}{\partial \theta} \end{vmatrix} = \begin{vmatrix} \cos\theta & c\sin\theta \\ -r\sin\theta & rc\cos\theta \end{vmatrix} = rc$$

and the operators for the derivatives are given by

$$\frac{\partial}{\partial x} \equiv \cos\theta \frac{\partial}{\partial r} - \frac{\sin\theta}{r}\frac{\partial}{\partial \theta} \quad (17a)$$

$$\frac{\partial}{\partial y} \equiv \frac{1}{c}\left(\sin\theta \frac{\partial}{\partial r} + \frac{\cos\theta}{r}\frac{\partial}{\partial \theta}\right) \quad (17b)$$

Using the above transformation (5) – (7) transform to the following equations:

$$\frac{\partial (cr\zeta)}{\partial t} + \frac{\partial}{\partial r}\{(\zeta + h)U\} + \frac{\partial}{\partial \theta}\{(\zeta + h)V\} = 0 \quad (18)$$

$$\frac{\partial \tilde{u}}{\partial t} + \frac{1}{cr}\left[\frac{\partial}{\partial r}(U\tilde{u}) + \frac{\partial}{\partial \theta}(V\tilde{u})\right] - f\tilde{v} = -g(\zeta + h)\left[\cos\theta \frac{\partial \zeta}{\partial r} - \frac{\sin\theta}{r}\frac{\partial \zeta}{\partial \theta}\right] + \frac{\tau_x}{\rho} - \frac{c_f \tilde{u}(u^2 + v^2)^{1/2}}{\zeta + h} \quad (19)$$

$$\frac{\partial \tilde{v}}{\partial t} + \frac{1}{cr}\left[\frac{\partial}{\partial r}(U\tilde{v}) + \frac{\partial}{\partial \theta}(V\tilde{v})\right] + f\tilde{u} = -g(\zeta + h)\frac{1}{c}\left[\sin\theta \frac{\partial \zeta}{\partial r} + \frac{\cos\theta}{r}\frac{\partial \zeta}{\partial \theta}\right] + \frac{\tau_y}{\rho} - \frac{c_f \tilde{v}(u^2 + v^2)^{1/2}}{\zeta + h} \quad (20)$$

where (21)

$$U = r[(c\cos\theta)u + (\sin\theta)v]$$

$$V = -[(\sin\theta)u + (C\cos\theta)v] \quad (22)$$

The boundary condition (10) - (12) transform to

$$V = 0 \ or \ -(g/h)^{1/2} \quad \text{at } \theta = \beta \quad (23)$$

$$V = 0 \ or \ (g/h)^{1/2} \quad \text{at } \theta = \alpha \quad (24)$$

$$U = K(g/h)^{1/2}\zeta \quad \text{at } r = K \text{ (no tide input)} \quad (25a)$$

$$U = K(g/h)^{1/2}\zeta - 2K(g/h)^{1/2} a \, Sin[(2\pi t)/T + \varphi] \quad \text{at } r = K \text{ (tide input)} \quad (25b)$$

Page 81-103 © MANTECH PUBLICATIONS 2019. All Rights Reserved

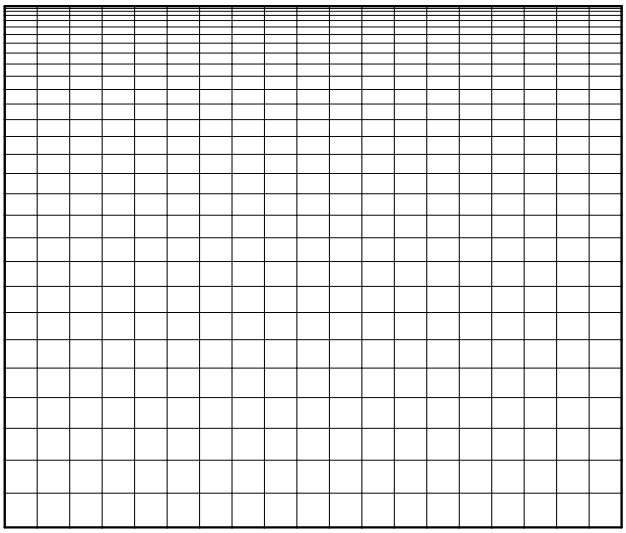


Figure 2b Rectangular grid system in the transformed domain.

FINITE DIFFERENCES SCHEME AND NUMERICAL SOLUTION

The choice of the present grid system ensures smaller meshes around the coastal belt as well as the offshore islands region and larger meshes away from the coast. As mentioned earlier the bounding lines of the physical domain is given by $y = m_1 x$ and $y = m_2 x$ where $m_1 = \tan\alpha$ and $m_2 = \tan\beta$. In the present study we consider $\alpha = 30°$ and $\beta = -60°$. The grid system is generated as the points of intersection of the pencil of $N_2 = 61$ straight lines $y = m\,x$ through O, including the above bounding lines, and the system of N_1 ellipses given by Eq.(14). In fact, we have considered a grid system where the angle between any two adjacent straight lines, given by $y = m\,x$, is taken as $\Delta\theta = 1.5°$.

- The north-south extent of the analysis area is 6^o (from 17^oN to 23^oN), which is approximately *667192.6* meters. If we generate N_1 concentric ellipses of fixed distant Δr (= the difference of any two adjacent ellipses along the semi-minor axes lying along x- axis) with $r = (n-1)\Delta r = 667192.6\ m$ where $n = 1, 2, 3, \ldots, N_1$. Thus, for $N_1 = 90$ grid points along radial direction, Δr should be *7496.546 meters.* The total number of grid points is then 90× 61.

- Now if we generate N_1 concentric ellipses of variable distant $(n-1)\Delta r$ with $r=\Sigma(n-1)\Delta r$ where $n = 1, 2, 3, \ldots, N_1$. For $N_1 = 30$ we have 30× 61 grid points for the same domain with $(0 + 1 + 2 + \ldots 29)\ \Delta r = 435\Delta r = 667192.6$ meters, thus $\Delta r = 1533.7761$ meters.

Page 81-103 © MANTECH PUBLICATIONS 2019. All Rights Reserved

This ensures that we can cover the same domain with a reduced number of grid points with more fine resolution near the origin or coast. Thus in the computational scheme there are 30 × 61 grid points of which 61 grid points meet at O. Since the origin O is at the land, no computation is done there and doesn't create any computational instability. The distant between any two adjacent grid points increases with the increase of r. Thus we have, actually, uneven resolution (small to big) as we move away from the coast. The coastal and island boundaries are now approximated along the nearest grid lines.

Let us define discrete coordinate points in the transformed domain by

$$r = r_i = \Sigma(i - 1)\,\Delta r, \qquad i = 1, 2, \ldots, N_1$$

$$\theta = \theta_j = (j - 1)\,\Delta\theta, \qquad j = 1, 2, \ldots, N_2$$

A sequence of time instant is given by

$$t = t_k = k\,\Delta t, \qquad k = 1, 2, 3, \ldots$$

In the computational domain we use staggered grid in which there are three distinct types of computational points. With i even and j odd, the point is a ζ- point at which ζ is computed. If i is odd and j is odd, the point is a u- point at which u is computed. If i is even and j is even, the point is a v- point at which v is computed. Since $N_1 = 30$ is even, there are ζ- points and v- points along the southern boundary. Similarly along each of the boundary lines $y = m_1x$ and $y = m_2x$, there are ζ- points and u- points. The coastal boundary is approximated either along the nearest odd elliptic grid line (i.e. i = odd), so that we have only u- points on this part of the boundary or along the nearest even straight grid line (i.e. j = even), so that we have only v- points along that part of the boundary.

Thus, the boundary of the coast is represented by such a stair step that, at each segment there exist only that component of velocity that is normal to the segment. This is done in order to ensure the vanishing of the normal component of velocity at the boundary in the numerical scheme. The governing equations (18) – (20) and the boundary conditions (23) – (25) are discretized by finite difference (forward in time and central in space) and are solved by conditionally stable semi- implicit method using staggered grid as mentioned earlier. For numerical stability, the velocity components in (19) and (20) are modeled in a semi-implicit manner. For example in the last term of (19) the time discretization of $\tilde{u}\,(u^2 + v^2)$ is done as

Page 81-103 © MANTECH PUBLICATIONS 2019. All Rights Reserved

$\tilde{u}^{k+1}(u^2 + v^2)^k$ where the superscript k and $k+1$ denote values at the present and advanced time levels respectively. Moreover, the CFL criterion has been followed in order to ensure the stability of the numerical scheme. Along the closed boundary, the normal component of the velocity is considered as zero, and this is easily achieved through appropriate stair step representation as mentioned earlier. The initial value of ζ, u, and v are taken as zero. The time step is taken as 30s, a uniform value of 0.0026 for the friction coefficient (C_f) and 0.0028 for the drag coefficient (C_D) are considered throughout the physical domain.

The coastal belt of Bangladesh has so many big and small offshore islands with a very high density around the Meghna estuary. It is possible to incorporate the small islands by considering very fine resolution of grids in the numerical scheme. There are some practical problems in considering very fine resolution viz. instability of the numerical scheme, more computing time, and very high memory etc. In this study since very high resolution is not ensured we are considering only three major islands and they are Sandwip, Hatiya and Moheshkhali (Cox's Bazar). Bhola is the biggest island and is located very near to the coastline; so it is considered as a part of main land.

RESULTS AND DISCUSSIONS

Analysis of the Computed Surge Response

The model is applied to compute the water levels due to tide and surge associated with a few tropical storms that hit the coast of Bangladesh. To analyze the result we have chosen the storms of November 2007 (Sidr) and May 2009 (Aila) with maximum sustained anti-clock wise circulatory wind velocities of 250 km/h (69.44 m/s) and 120 km/h (33.33 m/s) respectively. Table.1 gives the history of the above mentioned storms, the data of which was received from the Bangladesh Meteorological Department (BMD) (Figure 1).

For the purpose of analysis the computed results are presented at eight locations along the coast of Bangladesh. The storm of 2007 is one of the severe storms of this century that hit the coast of Bangladesh and is also favorable for high surge due to both wind intensity and path of its movement. So we give more stress on the 2007 storm data for computation of results.

Page 81-103 © MANTECH PUBLICATIONS 2019. All Rights Reserved

Table I. History of the chosen storms

Storm of 2007 (Sidr)				Storm of 2009 (Aila)			
Date	Hour	Lat.	Long.	Date	Hour	Lat.	Long.
1112	0600	10.8	90.4	0524	0000	18.1	88.5
1112	1200	11.0	90.3	0524	0600	18.4	88.4
1112	1800	11.6	90.0	0524	1200	18.3	88.4
1113	0000	12.1	89.9	0524	1800	19.1	88.2
1113	0600	12.5	89.8	0525	0000	20.3	88.1
1113	1200	13.0	89.6	0525	0600	21.6	88.3
1113	1800	13.7	89.5	0525	1200	22.9	88.2
1114	0000	14.3	89.6	0525	1800	24.2	88.5
1114	0600	15.0	89.4	0526	0000	24.2	88.5
1114	1200	15.7	89.3	0526	0600	24.2	88.5
1114	1800	16.6	89.3	0526	1200	27.1	89.2
1115	0000	17.8	89.2	0526	1800	27.1	89.2
1115	0600	19.3	89.3				
1115	1200	20.9	89.5				
1115	1800	22.8	90.3				
1116	0000	25.0	91.9				

Cyclone Sidr was one of the recent natural disasters along the Coast of Bangladesh. It was formed on November 11, dissipated on November 16, 2007. The peak sustained wind was 250 km/h. Red Crescent Society reported on November 18, 2007 that the number of deaths could be up to 10,000, total damages came close to $450 million. Sidr officially made landfall around 14:30 GMT, (about 08:30 p.m. local time) on 15 November with sustained winds of 215 km/h. The hardest-hit area was Barguna (Barishal) located near 22.9N degrees north latitude and 89.2E longitude. According to Bangladesh Meteorological Department (BMD) the entire area of Barishal division were hit hard by the storm surge of 5-7 meters (>16 ft).

Figure 3a, b depicts the computed surge levels associated SIDR at different coastal locations. It may be observed that, the maximum surge level is increasing with time as the storm approaches towards the coast and finally there is recession. At Hiron Point a strong recession is occurred after 14 hrs of 15th November, earlier than in any other locations and about 3 hrs before landfall of the storm. The recession takes place due to backwash of water from the shore towards the sea. In fact, Hiron Point is situated along left (west) of the storm path and so the direction of the anti-clock wise circulatory wind becomes northerly (i.e. towards the sea) at Hiron Point before the storm reaches the coast and thus driving the water towards the sea. The recession reaches up to -3.0 m approximately at 1700 hrs of 15th November. It may

Page 81-103 © MANTECH PUBLICATIONS 2019. All Rights Reserved

be noticed that the recession at Kuakata, Bhola, Hatiya, Char Jabbar, Chittagong and Cox's Bazar began later than Hironpoint (Figs. 3). Thus the beginning of recession delays as we proceed towards east as is expected. At every location, the peak surge is attaining before the land falls time of the storm. This is expected, as the circulatory wind intensity is highest along the coast when the storm reaches near the coast.

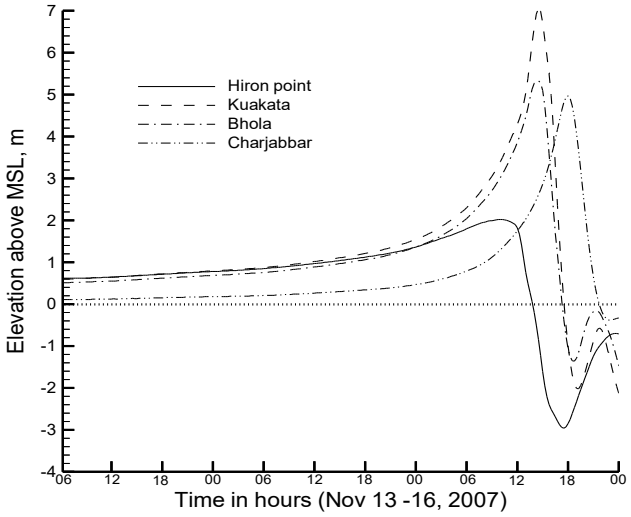


Figure 3a Computed time series of surge levels at the coastal locations associated with November 2007 storm (Sidr).

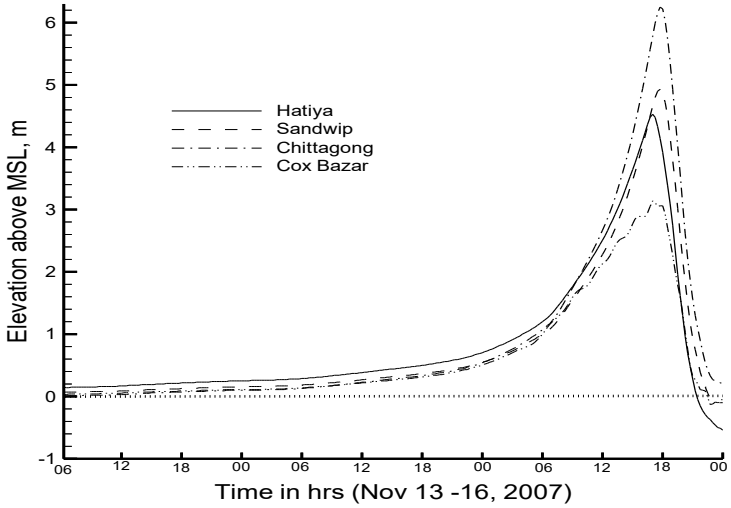


Figure 3b Computed time series of surge levels at the coastal locations associated with November 2007 storm (Sidr).

We could not compare our computed results to the observed data due to non availability of observed time series data. The Hydrographic department of BIWTA collects water level data

Page 81-103 © MANTECH PUBLICATIONS 2019. All Rights Reserved

at different coastal locations through manual gauge readers. During a severe storm period it is not possible to stay in the gauge station to collect the data, so observed time series data are not available. The results of the article are Explained and compared with the information obtained from the Institute of Water Modeling (IWM), Bangladesh Inland Water Transport Authority (BIWTA), Bangladesh Meteorological department (BMD) and the website of Wikipedia and NASA.

According to storm surge analysis by the Institute of Water Modeling (IWM), there was 4 to 7 meters surge along the coastal regions between Hiron point and Chittagong. Thus, the computed surge heights are almost identical with the report. Similar information about the water levels is found from Wikipedia website and the website of NASA.

Cyclone Aila was formed on May 23 and dissipated on May 26, 2009. The peak sustained wind was 120 km/h. Aila officially made landfall around 0800 UTC of 25 May 2009 with sustained winds of 110-120 km/h along the west of border area of Bangladesh and India. Figure 4a, b depicts the computed surge levels associated Aila at different coastal locations (without tidal consideration).

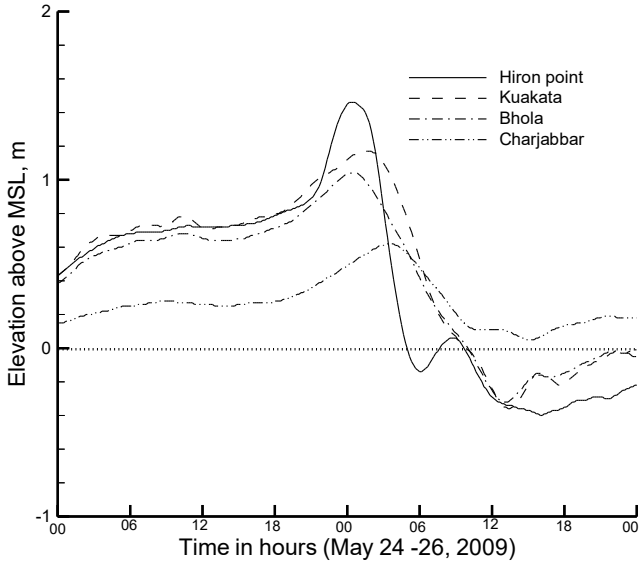


Figure 4a Computed time series of surge levels at the coastal locations associated with May 2009 storm (Aila).

Page 81-103 © MANTECH PUBLICATIONS 2019. All Rights Reserved

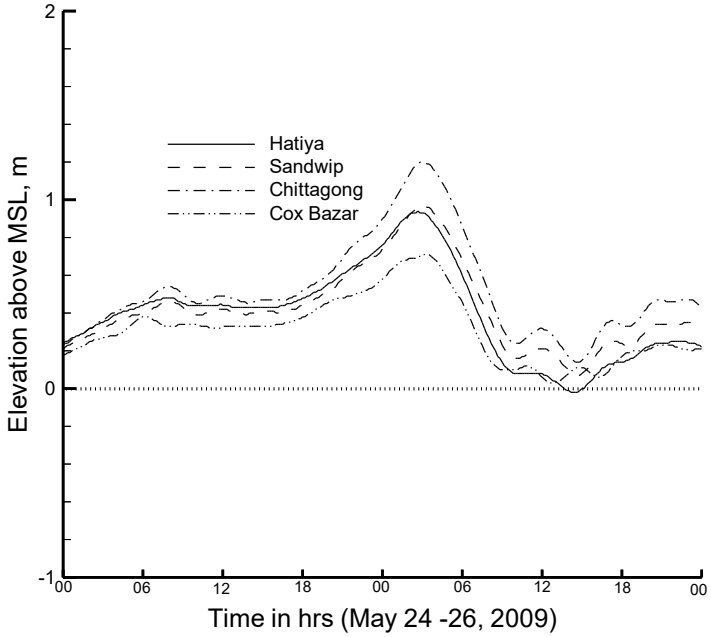


Figure 4b Computed time series of surge levels at the coastal locations associated with May 2009 storm (Aila).

It may be observed that, the maximum surge level is increasing with time as the storm approaches towards the coast and finally there is recession at Hironpoint. The recession is very low, because the entire Bangladesh coast is situated along the right of the storm path. According to storm surge analysis by the Institute of Water Modeling (IWM) Bangladesh, there was 3 to 5 meters surge along the coastal regions between Hiron point and Charjabbar of which 2 to 3 meter is due to the astronomical tide, because Aila made landfall at the time of high tidal period. The computed surge heights are almost in good agreement with the report of IWM. Same information about the water levels is found from Wikipedia website and the website of NASA.

Experiment is done to test the sensitivity of surge level with respect to the intensity of a storm. Figure 5a, b shows the peak surges along the coastal locations due to the storms of 2007 and 2009 respectively. The surge due to November 2007 storm is found to be much higher, which not only because of strong wind but also because of a favorable path for generating high surge (Table 1). It may be observed that, the coastal region between Barisal (Kuakata) and Chittagong is vulnerable for very high surge.

Page 81-103 © MANTECH PUBLICATIONS 2019. All Rights Reserved

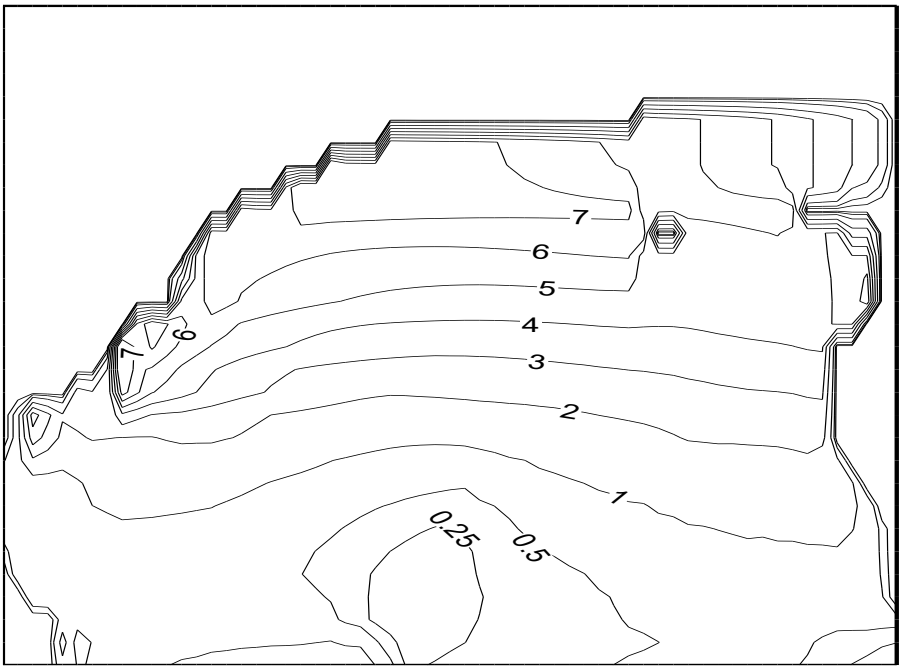


Figure 5a Peak surges along the coastal locations due to the storms of 2007 (Sidr).

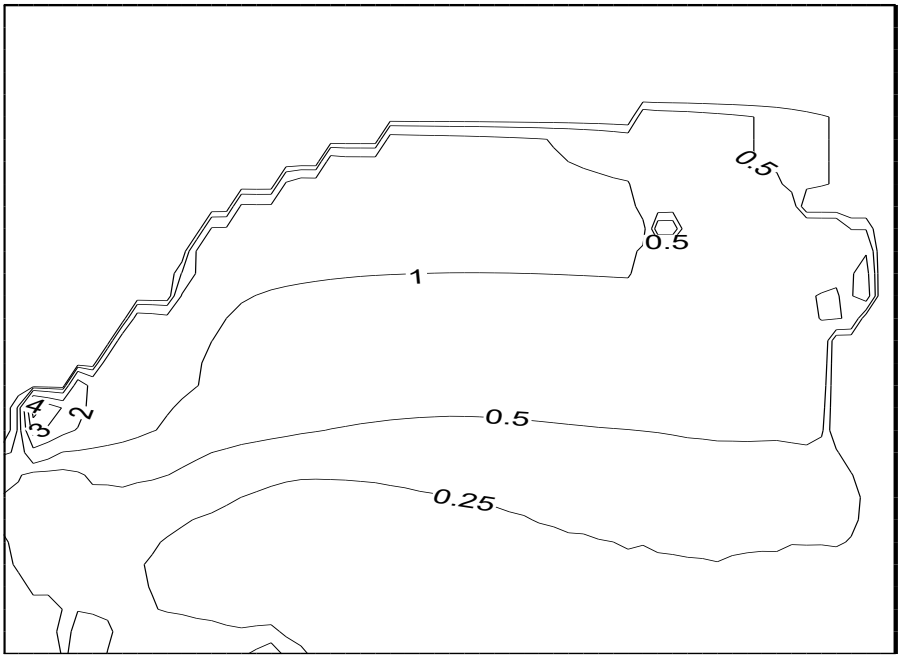


Figure 5b Peak surges along the coastal locations due to the storms of 2009 (Aila).

Analysis of the Computed Tide and Tide-Surge Interaction

We know, the astronomical tide is a continuous process in the sea, the surge due to tropical storms always interacts with the astronomical tide. So the pure tidal oscillation is the initial dynamical condition for interaction of tide and surge. A way of incorporating tidal oscillation

Page 81-103 © MANTECH PUBLICATIONS 2019. All Rights Reserved

with surge is to superimpose linearly the time series of surge response obtained through model simulation with that of oscillation obtain from tide table. The tidal information is generally available, as high and low values, four times a day in Bangladesh Tide Table.

The tide is generated in the model through the south open boundary condition (23b) with appropriate values of a, T, and φ in absence of wind stress. It is observed that, though there is variation in the tidal period in the head Bay of Bengal, the average period is approximately of M_2 tide and so we choose $T = 12.4$ hrs. By trial it is found that $\varphi = 0$ is a good choice for head Bay region. The information of the amplitude a along the southern boundary is not available.

We have chosen $a = 0.6\ m$ to test the response of the model along the coastal belt (Figure 6). It is found that response is exactly sinusoidal with the same period (12.4 hrs), which is expected. About the phase it may be seen in Figure 6b that the tide at all places are in the same phase of tidal oscillation except at Hiron point. This is because of the fact that, they are very close to each other. Hence providing appropriate values of the amplitude a along the southern open sea boundary condition the model may generate the actual tidal oscillation in the whole basin.

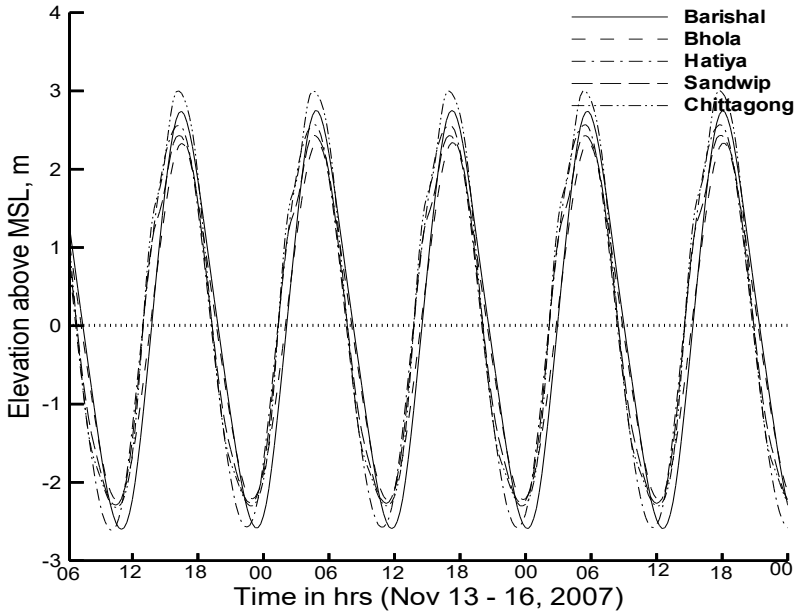


Figure 6a Computed tidal oscillations at different coastal locations.

Page 81-103 © MANTECH PUBLICATIONS 2019. All Rights Reserved

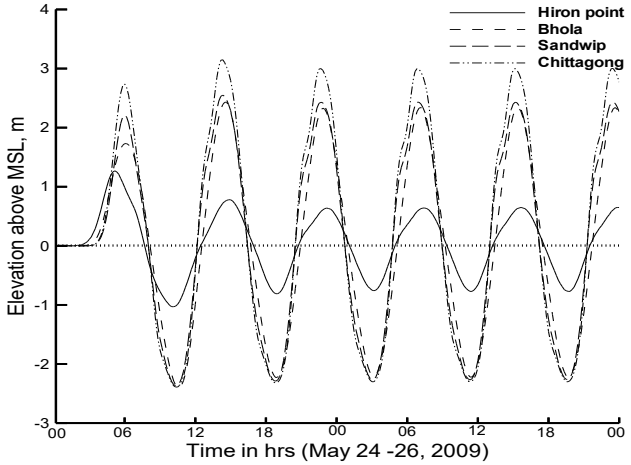


Figure 6b Computed tidal oscillations at different coastal locations.

Figure 7 shows the computed tide, computed surge, and their linear interaction associated with May 2009 storm at Kuakata, and Bhola. According to storm surge analysis by the Institute of Water Modeling (IWM), the computed water levels are quite satisfactory. The storm approaches the coast during high tide period and hence intensifies the water level due to interaction. At each location, because of weak wind the surge response is less when the storm is away from the coast and the total water level is dominated by tidal oscillation. On the other hand, because of very strong wind the water level is dominated by surge when the storm approaches the cost.

High tide is at approximately 1 a.m. local time and Sidr made landfall about halfway between low and high tide. For this reason, we are neglecting the tide and surge interaction for 2007 storm (Sidr) results.

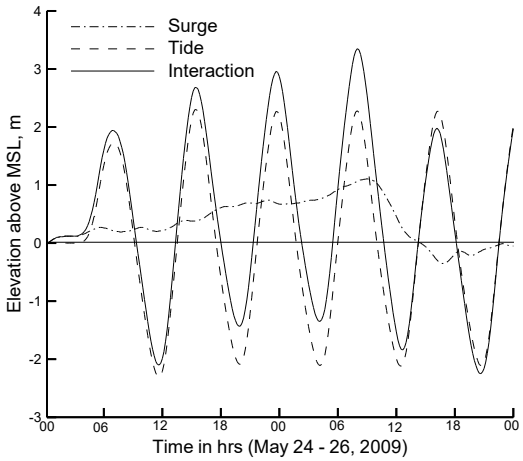


Figure 7a Computed tide, computed surge, and their linear interaction associated with May 2009 storm at Kuakata.

Page 81-103 © MANTECH PUBLICATIONS 2019. All Rights Reserved

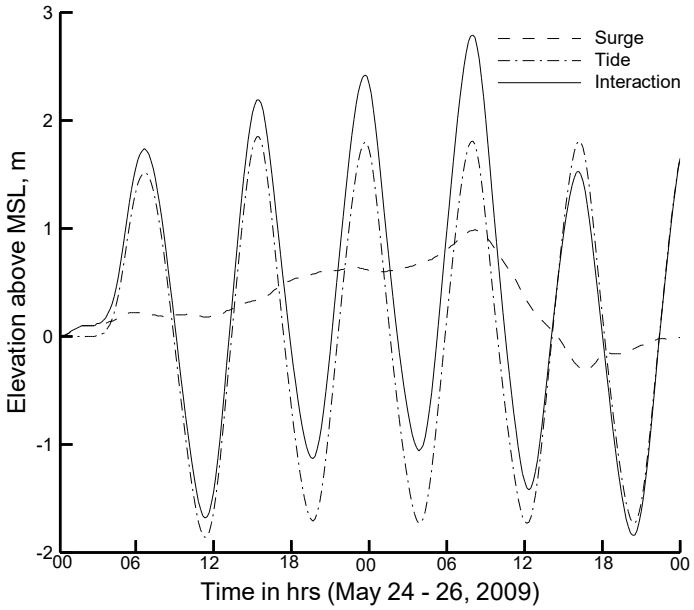


Figure 7b Computed tide, computed surge, and their linear interaction associated with May 2009 storm at Bhola.

CONCLUSION

In this study a new concept on grid generation has been developed which is very useful in incorporating the coastal and island boundaries in the head Bay of Bengal. This model should be simulated by using the authentic Oceanographic, Meteorological and Geographic data to test its efficiency. This concept of grid generation may further be extended to tackle more complicated boundaries as well as offshore islands.

ACKNOWLEDGEMENT

The author started her study in this field under the supervision of Professor Gauranga Dev Roy. Professor Roy was a great Bangladeshi scientist and researcher in the field of Atmospheric science. He died on 25th December 2008. The author is expressing her heartiest respect to the soul of Professor G. D. Roy by dedicating this article to him.

REFERENCES

I. Das, P. K., "Prediction model for storm surges in the Bay of Bengal", *Nature,* Vol. 239, pp. 211- 213, 1972.

II. Das, P. K., Sinha M. C., Balasubrahmanyam, V, "Storm surges in the Bay of Bengal", Quart *J. Roy. Met. Soc.* 100, 437- 449, 1974.

Page 81-103 © MANTECH PUBLICATIONS 2019. All Rights Reserved

III. Flierl, G. R., Robinson, A. R., "Deadly surges in the Bay of Bengal: Dynamics and storm tide tables", *Nature,* Vol. 239, pp. 213-215, 1972.

IV. Johns B., Ali, A., "The numerical modeling of storm surges in the Bay of Bengal", *Quart. J. Roy. Met. Soc.* Vol. 106, pp. 1-18, 1980.

V. M. M. Rahman, A. Hoque, G. C. Paul and M. J. Alam, "Nested Numerical Schemes to Incorporate Bending Coastline and Islands of Bangladesh and Prediction of Water Levels due to Surge", Asian *Journal of Mathematics and Statics,* Vol. 4, No. 1, pp. 21 -32, 2011.

VI. M. M. Rahman, A. Hoque, G. C. Paul, "A Shallow Water Model Water Model for the coast of Bangladesh and Applied to Estimate water levels for AILA", *Journal of Applied Sciences*, Vol. 11, No. 24, pp. 3821 -3829, 2011.

VII. M. M. Rahman, A. Hoque, G. C. Paul, "A Cyclone Induced Storm Surge Forecasting Model for the coast of Bangladesh with Application to the Cyclone Sidr", International *Journal of Mathematical Modelling and Computations*, Vol. 1 No. 2, pp. 77 -86, 2011.

VIII. Roy, G. D., "Estimation of expected maximum possible water level along the Meghna estuary using a tide and surge interaction model", *Environment International,* Vol. 21, No. 5, pp. 671- 677, 1995.

IX. Johns B. Dube, S. K. Mohanti, U. C., Sinha, P. C., "Numerical simulation of surge generated by the 1977 Andhra cyclone", Quart. *J. Roy. Soc. London,* Vol. 107, pp. 919-934, 1981.

X. Neetu Agnihotri, Chittibabu, P., Indu Jain, Rao, A. D., Dube, S. K., Sinha P. C., "A Bay-River Coupled Model for storm surge prediction along the Andhra coast of India", *Natural Hazards*, Vol. 39, pp. 83-101, 2006.

XI. Indu Jain, Neetu Agnihotri, Chittibabu, P., Rao, A. D., Dube, S. K., Sinha P. C., "Simulation of storm surges along Myanmar coast Using a location specific Numerical model", *Natural Hazards*, Vol. 39, pp. 71-82, 2006.

XII. Indu Jain, Rao, A. D., Dube, S. K., V. Jitendra, "Computation of Expected total water levels along the east coast of India", *Journal of coastal research*, Vol. 26, No 4, pp. 681-687, July 2010.

XIII. Dube, S. K., Indu Jain, Rao, A. D., T. S. Murty, "Storm surge modelling for the Bay of Bengal and Arabian sea", *Natural Hazards*, Vol. 51, pp. 3-27, 2009.

Page 81-103 © MANTECH PUBLICATIONS 2019. All Rights Reserved

XIV. Indu Jain, Chittibabu, P., Neetu Agnihotri, Dube, S. K., Rao, A. D., Sinha P. C., "Numerical Storm surge model for India and Pakistan", *Natural Hazards*, Vol. 42, pp. 67-73, 2007.

XV. Dube, S. K., Sinha, P. C., Roy, G. D., "The numerical simulation of storm surges along the Bangladesh coast", Dyn. *Atms. Oceans*, Vol. 9, pp. 121-133, 1985.

XVI. Dube S. K., Sinha, P. C., Roy, and G. D., "The numerical simulation of storm surges in Bangladesh using a bay-river coupled model", Coastal *Engineering*, Vol. 10, pp. 85-101, 1986.

XVII. Johnson, B. H., "Numerical modeling of estuarine hydrodynamics on a boundary fitted coordinate system", *Numerical Grid Generation* (Thompson, J., ed.) Elsevier, pp. 419 – 436, 1982.

XVIII. Johns B., Dube, S. K., Mohanti, U. C., Sinha, P. C.: The simulation of continuously deforming lateral boundary in problems involving the shallow water equations; *Computers and Fluids,* Vol. 10, pp. 105-116, 1982.

XIX. Roy, G. D., "Some aspects of storm surges along the coast of Bangladesh", *Ganith* (*J. Bangladesh Math. Soc.*), Vol. 6, No. 1, pp. 1- 8, 1985.

XX. Sinha, P. C., S. K. Dube, and G. D. Roy, "Numerical simulation of storm surges in Bangladesh using a multi-level model", *Int. J. for Num. methods in fluids,* Vol 6, pp. 305-311, 1986.

XXI. Roy G. D., "Inclusion of offshore islands in transformed coordinates shallow water model along the coast of Bangladesh", *Environment international,* Vol. 25, No. 1, pp. 67- 74, 1999.

XXII. Hussain Farzana, "A Transformed Coordinates Shallow Water Model for the Head of the Bay of Bengal using Boundary-Fitted Curvilinear Grids", East *Asian Journal on Applied Mathematics*, Vol 3, No 1, pp.27-47, February 2013.

XXIII. Roy G. D., Humayun Kabir, A. B. M., Mandal, M. M., Haque, M. Z., "Polar coordinate shallow water storm surge model for the coast of Bangladesh", *Dyn. Atms. Oceans,* Vol. 29, pp. 397- 413, 1999.

XXIV. Johns, B., Rao, A. D., Dube, S. K., Sinha P. C., "Numerical modeling of tide-surges interaction in the Bay of Bengal", Phil. *Trans. R. Soc. of London A*313, pp. 507-535, 1985.

XXV. Bao, X.W., Yan, J., Sun, W. X, "A three-dimensional tidal model in boundary-fitted curvilinear grids", *Estuarine, Coastal and Shelf Science* Vol. 50, pp. 775 – 788, 2000.

Page 81-103 © MANTECH PUBLICATIONS 2019. All Rights Reserved

XXVI. Sheng, Y. P., "On modelling three- dimensional estuarine and marine hydrodynamics", *Three- dimensional Models of Marine and Estuarine Dynamics* (Nihoul J. C.J, ed.) Elsevier Oceanography Series, Vol. 45, pp. 35 – 54, 1989.

XXVII. Spaulding, M. L., "A vertical averaged circulation model using boundary-fitted coordinates", *Journal of Physical Oceanography,* Vol. 14, pp. 973 – 982, 1984.

XXVIII. Thompson, J.F., Frank, C., Thames, F.C., Mastin, C.W., "Automatic numerical generation of body-fitted curvilinear systems for tied containing any number of arbitrary two-dimensional bodies", *Journal of Computational Physics*, Vol. 15, pp. 229-319, 1974.

XXIX. Debsarma, S. K., "Simulations of storm surges in the Bay of Bengal", *Marine. Geodesy*, Vol. 32, pp. 178-198, 2009.

XXX. Jelesnianski, C. P., "A numerical calculation of storm tides induced by a tropical storm impinging on a continental shelf", *Mon. Wea. Rev.* Vol. 93, pp. 343-358, 1965.

XXXI. http://en.wikipedia.org/wiki/Cyclone_Sidr

XXXII. http://www.nasa.gov/mission_pages/hurricanes/archives/2007/h2007_sidr.html

XXXIII. http://en.wikipedia.org/wiki/Cyclone_Aila

XXXIV. http://www.nasa.gov/mission_pages/hurricanes/archives/2009/h2009_aila.html

Page 81-103 © MANTECH PUBLICATIONS 2019. All Rights Reserved